This article has been accepted for publication in a future issue of this journal, but has not been fully edited. Content may change prior to final publication. Citation information: DOI 10.1109/TSG.2017.2703126, IEEE Transactions on Smart Grid

A Two-layer Energy Management System for Microgrids with Hybrid Energy Storage considering Degradation Costs

Chengquan Ju, *Student Member, IEEE,* Peng Wang, *Member, IEEE,*
Lalit Goel, *Fellow, IEEE* and Yan Xu, *Member, IEEE*

***Abstract*—The integration of renewable energy source (RES) and energy storage systems (ESS) in microgrids has provided potential benefit to end users and system operators. However, intermittent issues of RES and high cost of ESS need to be placed under scrutiny for economic operation of microgrids. This paper presents a two-layer predictive energy management system (EMS) for microgrids with hybrid ESS consisting of batteries and supercapacitors. Incorporating degradation costs of the hybrid ESS with respect to the depth of charge (DOD) and lifetime, long-term costs of batteries and supercapacitors are modeled and transformed to short-term costs related to real-time operation. In order to maintain high system robustness at minimum operational cost, a hierarchical dispatch model is proposed to determine the scheduling of utilities in microgrids within a finite time horizon, in which the upper layer EMS minimizes the total operational cost and the lower layer EMS eliminates fluctuations induced by forecast errors. Simulation studies demonstrate that different types of energy storages can be utilized at two control layers for multiple decision-making objectives. Scenarios incorporating different pricing schemes, prediction horizon lengths and forecast accuracies also prove the effectiveness of the proposed EMS structure.**

***Index Terms*—Optimization; microgrids; energy storage; energy management system (EMS); hierarchical control.**

NOMENCLATURE

A. Indices and suffixes

i	Storage device index.
t	Time index.
Δt	Time interval.
t_u, t_l	Time index in upper and lower layer.
$\Delta t_u, \Delta t_l$	Time interval in upper and lower layer.

B. State Variables

$P_M(t)$	Power of utility grid.
$P_B(t)$	Power of battery.
$P_{SC}(t)$	Power of supercapacitor.
$P_L(t)$	Power of load.
$P_{PV}(t)$	Power of PV.
$P_{WT}(t)$	Power of wind turbine.

This work was under the Adaptive Integrated Hybrid DC-AC Micro Power Parks System (ERIP04) program with Singapore Economic Development Board (EDB Singapore) and Energy Research Institute @ NTU (ERI@N). The authors would like to thank ERI@N for the financial support.

C. Parameters

DOD	Depth of discharge of battery.
$d_B(\Delta t)$	Depth of Charge of battery in Δt.
$E_{B.rated}$	Rated battery Capacity.
$E_B(t)$	Energy of battery at time t.
$E_{SC}(t)$	Energy of supercapacitor at time t.
η_{Bc}, η_{Bd}	Charging and discharging efficiency of battery.
η_{SCc}, η_{SCd}	Charging and discharging efficiency of supercapacitor.
a, b, c	Curve-fitting coefficients of battery lifetime.
$L_B(d_B)$	Battery lifetime with respect to $DOD = d_B$.
L_{SC}	Supercapacitor lifetime.
$E_{BA}(t)$	Actual capacity of battery at t.
$E_a(t)$	Accumulative energy of battery at t
C_B	Battery replacement cost.
C_{BAC}	Battery average degradation cost.
C_{BDC}	Battery degradation cost.
C_{SC}	Supercapacitor replacement cost.
C_{SCDC}	Supercapacitor degradation cost.
T_u, T_l	Length of prediction horizon in upper layer and lower layer.
$P_M^{\min}(t), P_M^{\max}(t)$	Power limits of utility grid.
$P_B^{\min}(t), P_B^{\max}(t)$	Power limits of battery.
$P_{SC}^{\min}(t), P_{SC}^{\max}(t)$	Power limits of supercapacitor.
$S_B^{\min}(t), S_B^{\max}(t)$	SOC limits of battery.
$S_{SC}^{\min}(t), S_{SC}^{\max}(t)$	SOC limits of supercapacitor.
$P_B^{\min}(t), P_B^{\max}(t)$	Power limits of battery.
$\sigma_B^l, \sigma_M^l, \sigma_{SC}^l$	Cost weighting coefficients.

I. INTRODUCTION

IN recent years, growing interest in renewable energy source (RES) has prompted microgrids to develop towards more intelligent and modernized entities. Microgrids integrate the distributed generators including conventional and renewable sources to supply predicted load of end-users in a decentralized manner [1]. However, intermittency and undispatchability of RES outputs induce system robust problems. Energy from RES might be unavailable due to bad weather conditions when electricity is needed [2]. Energy storage system (ESS) is usually integrated in microgrids to compensate power mismatch. ESS can also act as bidirectional mediators with the utility

This article has been accepted for publication in a future issue of this journal, but has not been fully edited. Content may change prior to final publication. Citation information: DOI 10.1109/TSG.2017.2703126, IEEE Transactions on Smart Grid

grid to store and export energy, providing auxiliary services and financial benefits for end-users based on various control strategies. In order to meet different operation requirements, the so-called hybrid ESS which combines different types of energy storage inherits advantages for each individual to provide an effective and reliable solution. Researches working on hybrid ESS in microgrids have covered from real-time operations that account for instant power sharing [3], [4] and frequency regulation [5], to scheduling problems that manifest charging strategies [6] and operational optimization in the long term [7], [8].

Previous studies for ESS-integrated microgrids have mostly featured on the design of energy management system (EMS) to improve energy efficiency and operation reliability of microgrids [9], [10]. Research in [11] decomposes the microgrid energy management into a unit commitment problem to account for voltage and frequency regulation and an optimal power flow problem to provide reactive power support. In [12], a heuristic method combined with a centralized EMS and local EMSs is proposed to determine ESS cycling operation at the household level. However, existing works have narrowly considered economic effects of the real-time ESS operation under different resources, load and environment conditions [13], and ignored or merely assumed a fixed price as the operational cost [1], [14]. Different from generation resources, the short-term dispatch for ESS has a significant impact on its lifetime in the long term. For example, battery life would be considerably deteriorated by frequent charging and discharging. On the other hand, the conflict of economy and security further complicate the optimal energy management in microgrids. Increasing the ESS capacity size will provide larger operating reserves to reduce the probability of loss of load, however at the expense of extra capital investment [15]. The two-fold requirements enforce the ESS operational cost to be accurately related to the long-term degradation process in real-time operation. However, the degradation cost of ESS was either neglected or modeled on a very rough and general basis in previous literature [16]–[18].

Hybridization of ESS further urges different dispatch decisions to be made given various operation targets and ESS characteristics. ESSs with large energy densities such as batteries are committed to exchange excess energy with other components and the utility grid, and those with large power ratings such as supercapacitors are used to compensate the instant power mismatch. Hence, in the face of different devices in the hybrid ESS, different time resolutions are required for the comprehensive design of EMS: the long-term time horizon manifests operational economy and the short-term time horizon reflects system security. To this end, this paper proposes a two-layer hierarchical EMS to account for the above considerations. The main contributions of this paper are addressed as follows:

1) A noval two-layer EMS for microgrid including the hybrid ESS is developed. Power dispatch is scheduled to minimize the operational cost in the upper layer, and forecast uncertainties and power fluctuations by RES are minimized in the lower layer.

2) The degradation cost models of battery and supercapacitor are developed to accurately reflect the explicit degradation process, bridging the long-term capital cost and the short-term operational cost for real-time economic dispatch.

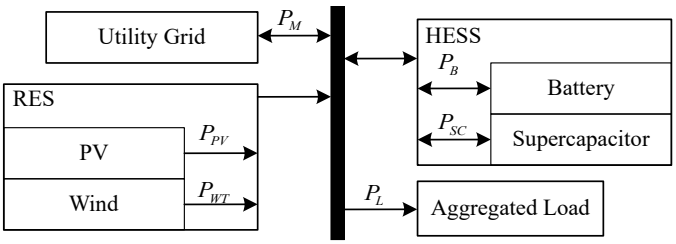

Fig. 1. System model of the microgrid.

3) The proposed EMS is applied to a microgrid presented in considering different electricity pricing mechanisms. The simulation studies successfully demonstrate that different types of energy storages including batteries and supercapacitors can be dispatched at different control layers for multiple decision-making objectives. Effectiveness of the proposed EMS structure is proved by various scenarios incorporating pricing schemes, prediction horizon lengths and forecast accuracies.

The remainder of this paper is organized as follows. In Section II, the microgrid modeling is proposed, and degradation cost models of battery and supercapacitor are presented respectively. Section III is focused on the formulation of the proposed two-layer EMS. Case studies and results are discussed in Section IV, in which the proposed two-layer EMS is simulated with selected scenarios. At last, the conclusion and main contributions of this paper are summarized in Section V.

II. Microgrid Modeling

A. Microgrid Structure

The schematic diagram of a typical microgrid is depicted in Fig. 1. Without loss of generality, the microgrid in our research is comprised of the point of common coupling (PCC) to the utility grid, a hybrid ESS, a RES system and the aggregate load. Practically, the microgrid can operate either in the grid tied mode or independently as an islanded grid, depending on system requirements, RES conditions and electricity market. Unless specified otherwise, we will focus on the grid connected mode in the following discussion.

B. Dynamic pricing

The utility grid is operated in an electricity market, where the electricity price is usually determined by the upper-level system operator in a static or dynamic way [19]. Static pricing schemes, such as fixed prices and time-of-use prices, are often set in advance and do not change with network conditions. Fixed prices do not usually influence user patterns in microgrid since the electricity cost does not change with the quantity of use, whereas time-of-use prices announced by the market authorities prompt more electricity to be used in off-peak hours considering relatively lower rates per kWh. Dynamic pricing schemes, such as the real-time pricing, are sensitive to locational marginal prices and are often announced hours

This article has been accepted for publication in a future issue of this journal, but has not been fully edited. Content may change prior to final publication. Citation information: DOI 10.1109/TSG.2017.2703126, IEEE Transactions on Smart Grid

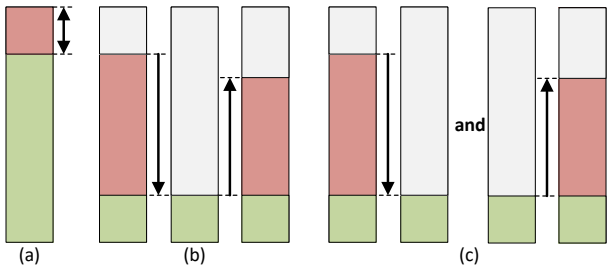

Fig. 2. Different definitions on DOD [22].

ahead, allowing users to make advanced scheduling so that the operational cost can be minimized [19]. When the bidirectional communication is allowed, microgrids can make profits by selling part of excess electricity to the utility grid.

Two pricing schemes, which are time-of-use pricing and dynamic real-time pricing, are adopted in this paper. In the time-of-use pricing model, the electricity price corresponds to a two-level model which has an off-peak value and an on-peak value. The specific values will be provided in Section V. In the dynamic real-time pricing model, the price is determined by the system operator according to the bidding of the market participants. In this paper, the half-hourly price data in EMA over a year is adopted to form the hourly data, starting from May 2013 to April 2014 [20]. Moreover, the selling price is also set in both pricing models, indicating the price per kWh that the microgrid sell extra generation back to the utility grid, which is lower than the buying price.

C. ESS Hybridization

Design features of the hybrid ESS vary in terms of power density, energy density, lifetime and cost [21]. In this paper, the hybrid ESS in the microgrid is comprised of the battery and supercapacitor given their complementary characteristics. The battery is able to store a large amount of electrical energy for the sake of high energy density, while the supercapacitor has high power density to give fast response for charging and discharging events. The main functions of the hybrid ESS include maintaining the instantaneous power balance and minimizing the operational cost over a period of time. Hence, the battery and supercapacitor should target different objectives, that the battery is scheduled to operate as the distributed generation unit for economic dispatch while the supercapacitor should make up the instant power mismatch.

D. Renewable Power Generation

The implementation of RES in the microgrid gives the EMS a more cumbersome task to track the instantaneous supply/demand balance. The microgrid is modeled with two RES systems including PV panels and wind turbines. PV generation is considered to have a great variation due to passing clouds. Wind power is closely correlated with wind speed, which follows different patterns on seasons and even days. RES forecast error is considered to have a close relationship with the prediction lead time. Solar power ranges from 20% to 35% root mean square (RMS) error depending on different irradiance forecast techniques. Day-ahead wind forecast currently averages at more than 10% RMS error of the capacity, and progressively reduces half to 5%-6% for one hour-ahead forecast [23]. Based on this fact, the RES output in this paper is modeled with a gradient uncertainty level, in which the forecast error increases when the receding horizon becomes larger. There are many existing and ongoing studies on RES forecasting methodologies, however, they will not be further discussed since different forecasting techniques are not within the scope of this paper.

III. Degradation Cost Modeling

The degradation of ESS is very important to evaluate economic operation of microgrid analytically [24]. In order to accurately model the cost properties for microgrid energy management, the degradation cost of the hybrid ESS is discussed and mathematically formulated in this section, especially for the battery and supercapacitor.

A. Modeling of Battery Degradation Cost

The degradation on battery lifetime features on two main factors, namely, the aging of cycle life that reflects the total achievable cycle count of a battery unit, and the capacity wear that accounts for the usable energy [25]. Cycling conditions, such as the number of frequent charging and discharging, charging and discharging rates and maintenance scheduling, have a great impact on the battery lifetime [26]. Improper cycling may cease to battery failure due to accelerated degradation. Apart from cycling conditions, state parameters also have significant influences on battery lifetime. Excessive high or low state of charge (SOC) would drastically deteriorate battery charging and discharging performance. Temperature may have a negative impact on the battery life as well, that at high temperatures the decay process will be accelerated. In practice, the temperature controller is often included in the battery management system. Therefore, it is assumed that the battery degradation due to ambient factors can be neglected. As for the effect of charging rate, its direct impact on battery lifetime is negligible in comparison of other parameters when battery is operating within a certain degree of rated current [27].

To this end, the primary determinants on battery lifetime are the actual full capacity and the depth of discharge (DOD). There are two main DOD definitions in the literature in accordance with different cycling events, as shown in Fig. 2(a) and (b). The first is the discharged energy from the full capacity (100% SOC), and the second refers to a full cycle consisting of one charging and discharging event [22]. Unless other specified in this paper, SOC is defined as the leftover energy compared to the full capacity, and DOD is defined as the energy in one charging or discharging event with respect to the full capacity, as illustrated in Fig. 2(c). We also define the actual full capacity of the battery as the amount of energy that can be stored at 100% SOC. Note that a cycle event is counted whenever the operating modes (charging and discharging) switch to the opposite sides.

This article has been accepted for publication in a future issue of this journal, but has not been fully edited. Content may change prior to final publication. Citation information: DOI 10.1109/TSG.2017.2703126, IEEE Transactions on Smart Grid

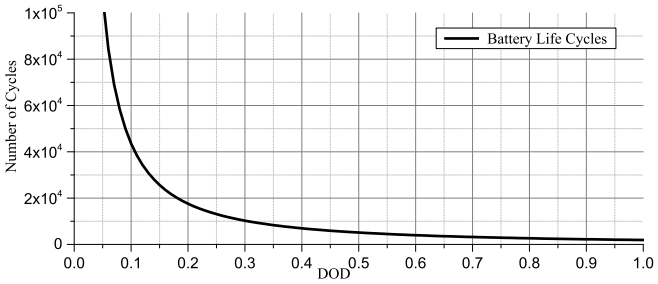

Fig. 3. Relationship of number of lifecycles and DOD of a Ni-Cd battery.

Fig. 3 shows a relationship between the number of life cycles and the DOD of Ni-Cd batteries [27]. The battery lifetime has the best fitting in the following expression with $DOD{=}d_B$:

$$L_B(d_B) = a \times {d_B}^{-b} \times e^{-cd_B} \tag{1}$$

where $a, b, c > 0$ are curve-fitting coefficients. As expected, the number of life cycles decreases with the increasing DOD. Without loss of generality, this expression is also applied for other types of batteries with different parameters such as Lithium-Ion and Lead-Acid batteries [28]. The statistical data is usually identified and provided by manufacturing specifications, however all charging and discharging cycles in the statistical data are assumed under conditions with constant DOD, which is apparently impractical in real-time operation. Therefore, estimation of battery degradation cost by using the above information would introduce gross errors. To the best of our knowledge, however, there is unfortunately no previous work featuring on direct relationships of variable DODs and battery lifetime. Therefore, in order to take the battery degradation cost model in a practical fashion, it is reasonably assumed that the empirical data of life cycles is accurate enough to estimate the long-term degradation effect, in other words, the effect of each charging and discharging cycle event on the lifetime is irrelevant with the historical charging and discharging profiles.

Given the actual capacity and DOD as two factors, the battery degradation model is based on the moderate assumptions:

a) The degradation process is considered to be time-linear throughout the whole battery life [29]; and

b) The degradation cost of each charging and discharging cycle event with the same level of DOD is the same at different levels of SOC.

The battery degradation cost model represents a direct depreciation on its actual capacity and lifetime. Considering a discharging event starting at time t with the average power $P_B(t)$ for a time interval Δt, the DOD during this interval, $d_B(\Delta t)$, can be expressed as:

$$d_B(\Delta t) = \frac{P_B(t)\Delta t}{E_{BA}(t)} \tag{2}$$

where $E_{BA}(t)$ is the actual capacity at time t. With the coefficients of charging/discharging efficiencies η_{Bc} and η_{Bd}, the average degradation cost per unit energy in this event in accordance with Fig. 3 can be formulated as follows [30]:

$$C_{BAC}\left(t, d_B(\Delta t)\right) = \frac{C_B \Delta t}{2L_B(d_B(\Delta t))E_{BA}(t)d_B(\Delta t)\eta_{Bc}\eta_{Bd}} \tag{3}$$

Note that it is a levelized degradation cost for each charging and discharging event with $DOD{=}d_B$. Therefore, we can get the corresponding battery degradation cost for this discharging event by simply multiplying the energy exported from the battery:

$$\begin{aligned} C_{BDC}\left(t, d_B(\Delta t)\right) &= C_{BAC}\left(t, d_B(\Delta t)\right) P_B(t) \\ &= \frac{C_B P_B(t)\Delta t}{2L_B(d_B(\Delta t))E_{BA}(t)d_B(\Delta t)\eta_{Bc}\eta_{Bd}} \end{aligned} \tag{4}$$

After the cycling event, the actual capacity of the battery at $t{+}\Delta t$ is proportionally deprecated, which can be calculated as follows:

$$E_{BA}(t + \Delta t) = E_{BA}(t) - \frac{E_{B.rated}}{L_B\left(d_B(\Delta t)\right)} \tag{5}$$

where $E_{B.rated}$ is the rated battery capacity.

In order to address the same degradation effect on the battery, we consider the cost of the charging event equal to that of the discharging event. Note that operation at too high or low SOC for a long time would in fact rise the internal impedance and decompose electrolyte in the battery, leading to capacity loss and power fade, however such fade in a short term would be insignificant compared with the degradation caused by chronic charging and discharging events. It is also noted that the effect of the charging and discharging rate on battery life will not be considered as a long-term effect as long as its current does not exceed the limit defined by manufacturer specifications, so as for other external parameters such as temperature and maintenance scheduling [30].

B. Modeling of Supercapacitor Degradation Cost

The lifetime of supercapacitor depends mostly on evaporation rate of liquid electrolyte, which is a principal function of temperature and terminal voltage [31]. In general, the lifetime of supercapacitor decreases with increasing central temperature. Supercapacitor is capable of undergoing thousands of deep cycles much more than battery and exhibits a much longer lifetime for more than ten years which is not limited by cycling stress [32]. Calendar ageing effects of supercapacitor are mainly resulted from voltage and temperature effects [33]. In particular, thermal conditions may have great influences on performance of supercapacitor, that capacitance degradation would be accelerated when the temperature is too high [34]. On the other hand, charging and discharging rates have little effect on superacapacitor degradation [35].

Since the supercapacitor lifetime at the maximum working temperature with proper voltage ranges is always given by manufacturing specifications, it can be reasonably assumed that supercapacitor is expected to last for the estimated life within normal operating conditions. Therefore, the supercapacitor degradation cost can be considered as a linear function of time despite of DOD of each charging/discharging event. Given the estimated supercapacitor lifetime L_{SC} and the

This article has been accepted for publication in a future issue of this journal, but has not been fully edited. Content may change prior to final publication. Citation information: DOI 10.1109/TSG.2017.2703126, IEEE Transactions on Smart Grid

replacement cost C_{SC}, the supercapacitor degradation cost for any time interval Δt can be simply presented as follows:

$$C_{SCDC}(t) = \frac{C_{SC}\Delta t}{L_{SC}} \tag{6}$$

(6) shows that different from the battery degradation cost, the supercapacitor degradation cost is constant irrespective of cycling conditions. Thus, the supercapacitor degradation cost is time-linear as long as it is utilized into microgrid. Therefore, it is more suitable for frequent charging/discharging to fill instantaneous power imbalance.

IV. Proposed Two-layer EMS

Based on the complementary characteristics of the battery and supercapacitor, in this section, a two-layer EMS is proposed to optimize the microgrid operation. Different from the two-layer structure formulated in the literature, such as in [36] that aims for energy loss minimization and in [37] which minimizes the averaged long-term cost, our proposed EMS achieves the minimal operational cost with the incorporation of the degradation model of hybrid ESS.

The objective of the proposed two-layer EMS is to optimize the power dispatch of power sources and energy resources in a finite period of time, so that the microgrid operates economically while satisfying operational limits under RES uncertainties. We consider a discrete-time optimization problem incorporated with the model predictive control framework, since the forecast uncertainty can be potentially compensated due to feedback mechanism [16], [38]. Fig. 4 illustrates the hierarchical structure of the proposed two-layer EMS, in which in which T_u and T_l denote the length of prediction horizon in the upper and lower layer, respectively. The upper layer EMS consists of a nonlinear receding model predictive controller with the time horizon $t_l \in \{1, ..., T_l\}$, and the lower layer EMS is a quadratic model predictive controller with the time horizon $t_u \in \{1, ..., T_u\}$. Δt_u and Δt_l indicate the time intervals in the upper and lower layer, respectively.Control actions in each time interval are obtained by solving its own objective function in each layer that the decisions of one layer influence those of the other. At current time, the optimal scheduling is formulated for T_u in the upper layer based on the predictions of the upcoming load profile, renewable outputs and electricity prices, however only the dispatch within the time frame $T_l\Delta t_l + \Delta t_u$ will be implemented as the reference values to control dispatch actions at the lower layer. Then, the lower layer EMS makes its own optimization with the implementation of supercapacitor, which is to minimize power fluctuations after the realization of forecast errors in each ΔT_l within the low-layer horizon T_l. After time Δt_u, the lower layer EMS sends the updated state variables back to the upper layer, and the scheduling problem will start for the next ΔT_u.

A. Mathematical Model for State Dynamics and Constraints of ESS

For both upper and lower layer, the power balance constraints must be meet at all times, which can be formulated as follows:

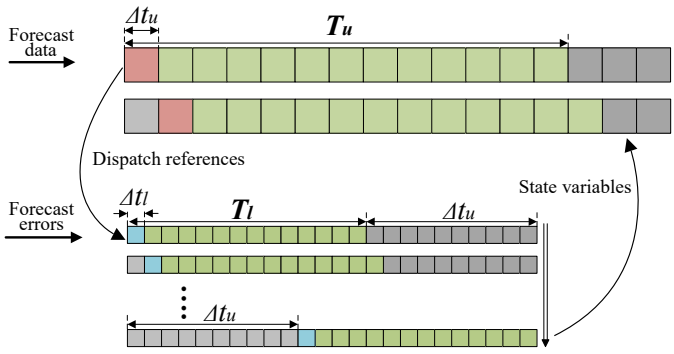

Fig. 4. Structure of the proposed two-layer EMS.

$$\underbrace{P_L(t)}_{Load} = \underbrace{P_M(t)}_{Utility\ grid} + \underbrace{P_B(t) + P_{SC}(t)}_{ESS} + \underbrace{P_{PV}(t) + P_{WT}(t)}_{RES},\ t \in \{t_u, t_l\} \tag{7}$$

State dynamics must be specified for both the battery and supercapacitor in terms of capacities and charging/discharging power for two time horizons. Let $P_B(t)$ and $P_{SC}(t)$ denote the power of battery and supercapacitor, respectively. Considering charging and discharging efficiencies, the discrete-time capacity difference equations of the battery and supercapacitor can be presented as follows, respectively:

$$E_B(t) = \begin{cases} E_B(t-1) - P_B(t)\Delta t\eta_{Bc}, P_B(t) \le 0 \\ E_B(t-1) - \dfrac{P_B(t)\Delta t}{\eta_{Bd}}, P_B(t) > 0 \end{cases}, \quad \Delta t \in \{\Delta t_u, \Delta t_l\},\ t \in \{t_u, t_l\} \tag{8}$$

$$E_{SC}(t) = \begin{cases} E_{SC}(t-1) - P_{SC}(t)\Delta t_l\eta_{SC}, P_{SC}(t_l) \le 0 \\ E_{SC}(t-1) - \dfrac{P_{SC}(t)\Delta t_l}{\eta_{SCd}}, P_{SC}(t_l) > 0 \end{cases} \tag{9}$$

The inequality constraints include power capacity limits of the utility grid, battery and supercapacitor as follows, respectively:

$$P_M^{\min}(t) \le P_M(t) \le P_M^{\max}(t),\ t \in \{t_u, t_l\} \tag{10}$$

$$P_B^{\min}(t) \le P_B(t) \le P_B^{\max}(t),\ t \in \{t_u, t_l\} \tag{11}$$

$$P_{SC}^{\min}(t_l) \le P_{SC}(t_l) \le P_{SC}^{\max}(t_l) \tag{12}$$

To prevent the battery from being overcharged and overdischarged, its SOC limit is expressed as follows:

$$S_B^{\min}(t) < \frac{E_B(t)}{E_{BA}(t)} < S_B^{\max}(t),\ t \in \{t_u, t_l\} \tag{13}$$

Accordingly, the supercapacitor SOC limit is expressed as follows:

$$S_{SC}^{\min}(t) < \frac{E_{SC}(t)}{E_{SC.rated}} < S_{SC}^{\max}(t),\ t \in \{t_u, t_l\} \tag{14}$$

Note that the scheduling of supercapacitor will not be actually included in the upper layer due to its low capacity, therefore, the state dynamic in (9) and the power constraint

in (12) are only considered in the lower layer. The lower boundary of $P_M(t)$ is negative when the microgrid is allowed to sell electricity to the utility grid.

B. Mathematical Model for Upper Layer EMS

With the aforementioned models in Section III, the objective of the upper layer EMS is to optimize the decision variables $\{P_M(t_u), P_B(t_u)\}_{t_u=1}^{T_u}$ to minimize the total operational cost, including electricity cost of the utility grid and and battery degradation cost.

The electricity cost $C_M^u(t_u)$ can be presented as follows:

$$C_M^u(t_u) = c_m(t_u) P_M^u(t_u) \Delta t_u \tag{15}$$

Since the battery degradation cost $C_B^u(t_u)$ in each time interval Δt can be determined only after when a charging or discharging event has ended, the power flow direction of the battery $P_B(t_u)$ must be specified. To this end, we firstly denote $g(t_u)$ to be an auxiliary binary variable to indicate the state transition on the charging and discharging events in two consecutive time intervals:

$$g(t_u) = \begin{cases} 1, \ if \ P_B(t_u) P_B(t_u - 1) \le 0 \\ 0, \ if \ P_B(t_u) P_B(t_u - 1) > 0 \end{cases} \tag{16}$$

We also denote $E_a(t_u)$ as the accumulative energy in kWh before the cycling events have been changed. Correspondingly, the accumulative energy $E_a(t_u)$ can be written as follows:

$$E_a(t_u) = (1 - g(t_u))\, E_a(t_u - 1) + P_B(t_u) \Delta t_u \tag{17}$$

Therefore, the battery degradation cost in the consecutive time intervals can be presented by the state transition signal $g(t_u)$ the accumulative energy $E_a(t_u)$ as follows:

$$\begin{aligned} C_B^u(t_u) = {} & C_{BDC}(t_u, \frac{E_a(t_u)}{E_B(t_u)}) \\ & - (1 - g(t_u))\, C_{BDC}\left(t_u, \frac{E_a\,(t_u - 1)}{E_B\,(t_u - 1)}\right) \end{aligned} \tag{18}$$

Combining the electricity cost and the battery degradation cost in the objective function,

the optimization problem in the upper layer EMS is a nonlinear programming problem since the battery degradation cost is highly nonlinear. The optimization problem F_u can be formulated as follows:

$$\begin{aligned} F_u : \min \ & \sum_{t_u \in \{1,\ldots,T_u\}} C_M^u(t_u) + \sum_{t_u \in \{1,\ldots,T_u\}} C_B^u(t_u) \\ \text{s.t. } & (7), (8), (10), (11), (13) - (18) \\ \text{variables} : \ & \{P_M(t_u), P_B(t_u)\}_{t_u=1}^{T_u} \end{aligned} \tag{19}$$

C. Mathematical Model for Lower Layer EMS

The objective of the lower layer EMS is to optimize the decision variables $\{P_M(t_l), P_B(t_l), P_{SC}(t_l)\}_{t_l=1}^{T_l}$ so that the variation resulted from forecast errors with the implementation of supercapacitor can be minimized. Considering (6) that the supercapacitor degradation cost is a function only related with time, the supercapacitor degradation cost $C_{SC}^l(t_l)$ can be writern as follows:

$$\sum_{t_l \in T_l} C_{SC}^l(t_l) = \frac{C_{SC}}{L_{SC}} T_l \tag{20}$$

It can be easily observed the supercapacitor degradation cost is independent with the charging/discharging power.

Accordingly, aside from the supercapacitor degradation cost, penalty costs that represent deviations from references provided by the upper layer EMS are added into the objective function. These penalty terms are denoted as $C_B^l(t_l)$ and $C_M^l(t_l)$ that represent the deviations on power references of the battery and utility grid due to forecast errors of RES in short-time scales. Given the power references from the upper layer, the penalty costs can be formulated as a quadratic function:

$$C_B^l(t_l) = (P_B^u(t_u) - P_B^l(t_l))^2 \tag{21}$$

and

$$C_M^l(t_l) = (P_M^u(t_u) - P_M^l(t_l))^2 \tag{22}$$

In addition, at the end of each prediction horizon, the SOC of supercapacitor should be maintained at a nominal value such that it is able to provide ramping services in the coming future. Hence, the penalty term $C_{SC}^l(T_l)$ that accounts for the capacity of supercapacitor in the prediction horizon terminal can be also presented as a quadratic function:

$$C_{SC}^l(T_l) = (E_{sc}^u(t_u) - E_{SC.rated})^2 \tag{23}$$

Combining the above quadratic factors in the objective function and convex constraints, the optimization problem in

1: Initialize $t_u = 1$
2: **for** $t_u = 1$ **to** T_u, **do**
3: Import the forecast data of load and renewables $[P_L(t_u), P_{PV}(t_u), P_{WT}(t_u)]_{t_u}^{t_u+T_u}$
4: Optimize F_u in *upper layer*
5: Make decision variables $[P_B(t_u), P_M(t_u)]_{t_u}^{t_u+T_u}$ within $T_l \Delta t_l + \Delta t_u$ for the lower layer as set points
6: **for** $t_l = 1$ **to** T_l, **do**
7: Import the forecast data of load and renewables with errors $[P_L(t_l), P_{PV}(t_l), P_{WT}(t_l)]_{t_l}^{t_l+T_l}$
8: Optimize *lower layer* objective function F_l
9: Dispatch power of $[P_M(t_l), P_B(t_l), P_{SC}(t_l)]_{t_u+t_l}$
10: **end for**
11: Return state variables $[E_B(T_l), E_{SC}(T_l)]_{t_u+1}$ to the upper layer
12: **end for**

Fig. 5. Algorithm of control strategy for two-layer EMS.

This article has been accepted for publication in a future issue of this journal, but has not been fully edited. Content may change prior to final publication. Citation information: DOI 10.1109/TSG.2017.2703126, IEEE Transactions on Smart Grid

the lower layer can be formulated as a quadratic programming problem as follows:

$$\begin{aligned} F_l: \ \min \ & \Big(\sum_{t_l \in \{1,\dots,T_l\}} C^l_{SC}(t_l) \\ & + \sum_{t_l \in \{1,\dots,T_l\}} \Big(\sigma^l_B C^l_B(t_l) + \sigma^l_M C^l_M(t_l) \Big) \\ & + \sigma^l_{SC} C^l_{SC}(T_l) \Big) \\ \text{s.t. } & (8), (9), (10), (11) - (14), (20) - (23) \\ \text{variables}: \ & \{P_M(t_l), P_B(t_l), P_{SC}(t_l)\}_{t_l=1}^{T_l} \end{aligned} \tag{24}$$

where σ^l_B, σ^l_M and σ^l_{SC} are cost weighting coefficients.

D. Remarks

In summary, the control strategy of the proposed two-layer EMS is outlined in Fig. 5. As illustrated in (19) and (24), the upper layer EMS minimizes the total operational cost including the electricity and degradation cost, and passes decision variables $[P_B(t_u), P_M(t_u)]$ to the lower layer as references. Considering load fluctuations and RES forecast errors, the optimization process is executed for each time interval ΔT_l, and the scheduling in the lower layer is made thereafter. After all the dispatch decisions within Δt_u have been made, the upper layer updates state variables $[E_B(T_l), E_{SC}(T_l)]$ and starts the scheduling for $t_u = t_u + 1$.

The optimization problem F_u in the upper layer is a nonlinear mixed-integer problem, as the cost function involved battery degradation cost $C^u_B(t_u)$ is nonlinear and includes integer terms. Similarly, the optimization problem F_l in the lower layer is a quadratic mixed-integer problem. There have already been many mature and advanced solvers with various algorithms so far that can handle to solve algebraic models with converged results, therefore comparison of their performances will not be further discussed since it is out of the scope of this paper.

It should be noted that in the lower layer, the supercapacitor may sometimes reach the capacity limit in the circumstances when the RES has increasingly excessive output. Since the upper layer EMS strives to maintain the battery output constant, it is necessary to conduct a new dispatch for all the components in the upper layer EMS in order not to violate the supercapacitor constraints.

V. Performance Evaluation

A. Simulation Setups

In this section, the proposed two-layer EMS associated with degradation cost models is demonstrated in three cases under different scenarios including pricing schemes, prediction horizons and forecast errors, and its performance is evaluated with several existing algorithms. The mathematical model described above as implemented in Matlab and optimization problem in the upper and lower layer is solved using the solver IPOPT [39] and Gurobi [40] integrated with Matlab, respectively.

The parameters in the case studies are listed in Table I. The simulation is conducted for a 48h scheduling horizon, and the time intervals in the upper and lower layer are set to be 1h and 5min, respectively. The exact power of load, PV and wind turbine are shown in Fig. 6. The parameters of hybridized ESS are shown in Table II. The battery is set to have a capacity of 12kWh at 600$ per kWh and the maximum power of 4kW. The charging and discharging efficiencies are both 95%, and the SOC operation range is set to be 10% to 90%. Its DOD-cycle curve is obtained so that the coefficient (a, b, c) takes the values of (4980,1.98,0.016), respectively [27]. The capacity and maximum power of supercapacitor is set to be 1kWh and 10kW, respectively, with its charging and discharging efficiency at 92% [41], [42].

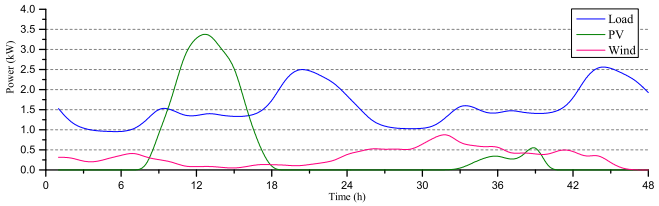

Fig. 6. Exact power of load, PV and wind turbine in 48 hours.

TABLE I
Parameters in Case Studies

Case	pricing scheme	forecast error	prediction horizon		time interval	
			T_u	T_l	Δt_u	Δt_l
1	**time-of-use**	5%-10%	48	12	1h	5min
	real-time					
2	time-of-use	5%-10%	**6-96**			
3	time-of-use	5%-(**10%~40%**)	48			

Time-of-use: the electricity price is set as 0.1$/kWh during off-peak hours (hour 0-8 and 18-23) and 0.25$/kWh at on-peak hours (hour 9-17).

Real-time: the hourly data is adopted by weighting the half hourly data from May 2013 to April 2014 in Energy Market Company of Singapore [20].

TABLE II
Parameters of Hybridized ESS

Type	Price ($/kWh)	Capacity (kWh)	Power (kW)	S^{min}	S^{max}	η_c	η_d	Coefficients		
								a	b	c
battery	600	12	4	10%	90%	95%	95%	4980	1.98	0.016
suparcap	3600	1	10	0%	100%	92%	92%	N.A.		

In case 1, the time-of-use pricing and real-time pricing are implemented in two scenarios, respectively. In the time-of-use pricing, the electricity price is set as 0.1$/kWh during off-peak hours (hour 0-8 and 18-23) and 0.25$/kWh at on-peak hours (hour 9-17). In the real-time pricing, the hourly data is adopted by weighting the half hourly data from May 2013 to April 2014 in Energy Market Company of Singapore [20]. The selling price is set as 80% of the electricity price in both pricing schemes. In case 2, six time lengths of the prediction horizon in the upper layer EMS from 6h to 96h are selected, respectively. In case 3, variable RES forecast errors are adopted with the standard deviation from 10% to 40% at the time terminal in the upper layer.

B. Case Studies

1) Different Pricing Schemes: The results of the optimal dispatch based on time-of-use pricing by the proposed EMS are shown in Fig. 7a. As expected, the operation of the battery

This article has been accepted for publication in a future issue of this journal, but has not been fully edited. Content may change prior to final publication. Citation information: DOI 10.1109/TSG.2017.2703126, IEEE Transactions on Smart Grid

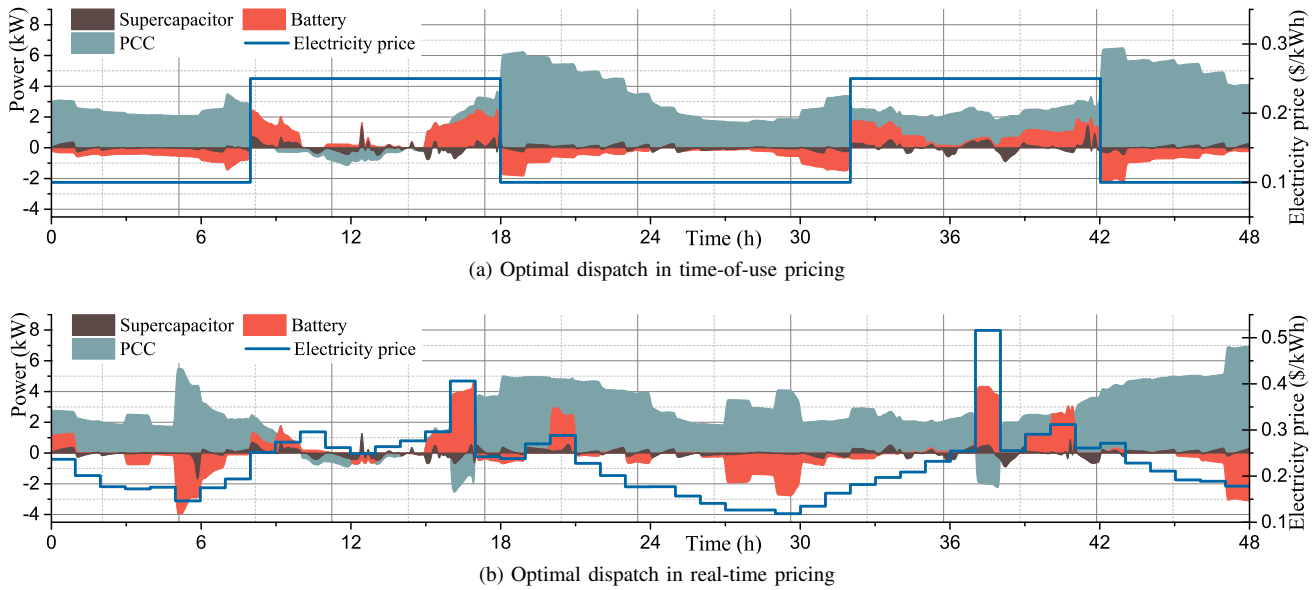

Fig. 7. Case 1: results of two scenarios with different pricing schemes.

is mainly scheduled by the electricity price in the upper layer EMS, in which the battery is charging during off-peak hours and discharging during on-peak hours. In addition, excessive energy generated by the RES at hour 11 to 13 is sold back to the utility grid since the electricity price is high. Similar results with the real-time pricing scheme are illustrated in Fig. 7b. In addition, it is observed that the battery has sensitive responses to high electricity prices at hour 16, 20 and 37 when the battery is quickly discharged. When the electricity price is relatively lower at hour 17 and 18, the battery is charged to ensure enough energy can be discharged in next following hours. On the other hand, it can be also observed in Fig. 7 that the lower layer EMS handles the fluctuation within each hour, that the power variations of the utility grid and battery have been stabilized within small ranges while the supercapacitor is frequently charged and discharged at a large rate to flatten the load uncertainties and forecast errors.

2) Impact of Prediction Horizons: Fig. 8 shows the results of six scenarios with different prediction horizons from 6h to 96h. It is indicated in Fig. 8a that the SOC of battery varies with the changing prediction horizon. When it increases over 24h, the battery SOC change becomes much less significant. The operational cost and the battery degradation cost are depicted in Fig. 8b and Fig. 8c, showing that high levels of detail on prediction horizon result in less variation on costs. Typically, the variation on the system operational cost is reduced when the prediction horizon reaches 24h, because the load profile follows similar daily patterns. It is also illustrated in Fig. 8d that despite of the length of prediction horizon, the average operational cost in 48 hours does not have great changes with different prediction horizon, whereas a significant decrease on the battery degradation cost has taken place.

Table III shows the average computation time with different prediction horizons. It can be reasonably observed that with the larger prediction horizon setting the computation time of upper layer increases while that of lower layer remains nearly same. However, the two-layer EMS ensures the optimal results to be obtained before the next upcoming time slot, since the computation time is much shorter than the corresponding time interval. It is thus clearly shown that that the computation ability is quite sufficient for the system needs.

TABLE III
AVERAGE COMPUTATION TIME OF DIFFERENT PREDICTION HORIZONS

prediction horizon	computation time (s)	
	upper layer	lower layer
6h	2.989	2.247
12h	6.732	2.263
24h	12.931	2.182
48h	20.688	2.239
72h	32.433	2.430
96h	50.978	2.305

3) Impact of Forecast Accuracies: Fig. 9 shows the results of four scenarios with increasing forecast errors from 10% to 40%. It is indicated in Fig. 9a that battery operation does not change very much with increasing forecast errors, whereas the supercapacitor output has been influenced to a great extent as shown in Fig. 9b. It can be also observed that the supercapacitor output is mainly affected in the daytime when solar energy is more abundant and intermittent, resulting into relatively more uncertainties on RES outputs. Since one major objective of the lower layer EMS is to smooth the battery output, it is reasonably explained that increasing forecast errors introduces more volatile variations on the supercapacitor output. On the other hand, the operation of supercapacitor is regulated by the lower layer EMS, which is responsible for instantaneous power mismatch, leading to the fact in Fig. 9c that neither the total operational cost nor the battery degradation cost has any significant change with increasing forecast errors.

This article has been accepted for publication in a future issue of this journal, but has not been fully edited. Content may change prior to final publication. Citation information: DOI 10.1109/TSG.2017.2703126, IEEE Transactions on Smart Grid

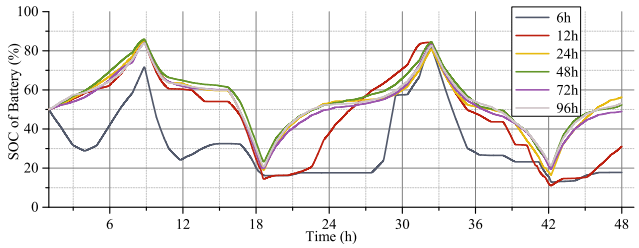

(a) SOC of battery

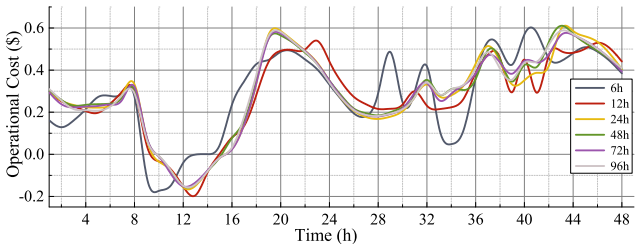

(b) Operational cost

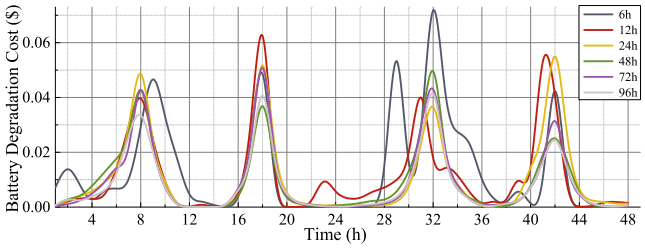

(c) Battery degradation cost

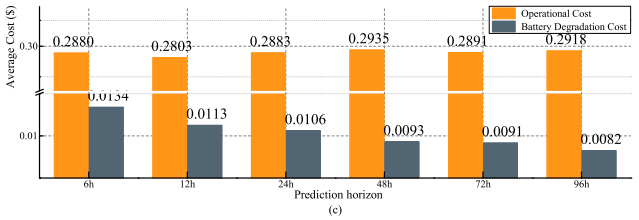

(d) Hourly average cost

Fig. 8. Case 2: results of six scenarios with different prediction horizons.

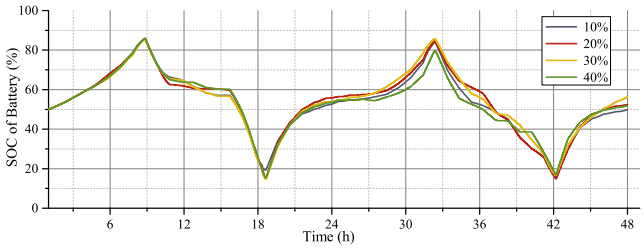

(a) SOC of battery

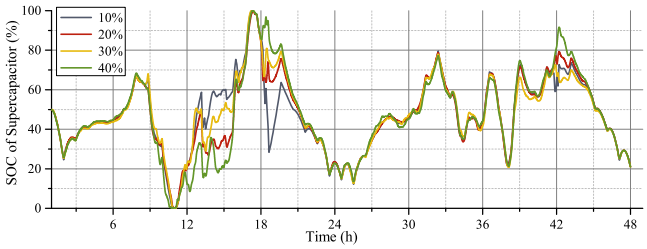

(b) SOC of supercapacitor

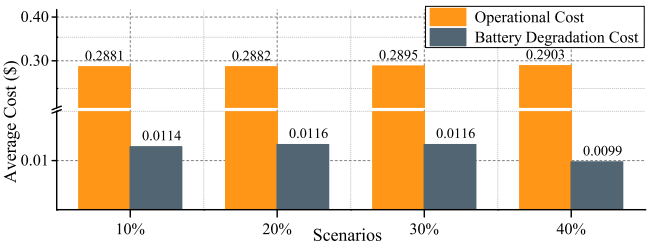

(c) Hourly average cost

Fig. 9. Case 3: results of four scenarios with different forecast errors.

TABLE IV
COMPARISON BENCHMARKS

Battery cost model	Algorithm
I: proposed battery degradation cost	A: proposed two-layer EMS
II: fixed battery degradation cost [27], [43]	B: single logic control
III: 5-level piece-wise linear cost	C: centralized EMS [11]
IV: 9-level piece-wise linear cost	
V: quadratic cost [18]	

C. Comparison with Benchmarks

In order to evaluate the performance and advantages of the two-layer EMS with the degradation cost models, several benchmark approaches and algorithms in the literature are analyzed. All the comparative scenarios are summarized in Table IV.

For comparison with the proposed nonlinear battery cost models, Four other scenarios are simulated arbitrarily for the case 1 with the time-of-use pricing scheme in Table I. The fixed battery degradation cost per kWh is calculated from purple(3) by using the averaged DOD d_B = 60% as a regular basis (SOC from 80% to 20%) [27], [43]. The 5-level and 9-level piece-wise linear models are generated by averaging the battery degradation cost from 0% to 100%, respectively. The quadratic cost in [18] and is also incorporated for a more comprehensive comparison.

To further illustrate the advantages of the proposed two-layer operation structure, two different control algorithms with the the single-layer structure are added into the benchmarks. The single logic control is deployed in which the whole hybridized ESS operates in just one layer. The battery will be charged or discharged as long as it is available, while the supercapacitor only accounts for mitigation of mismatches between load and PV outputs. The centralized EMS structure in [11] with the same solver of the proposed algorithm is tested as well.

Table V shows the results of the comparative cases for all scenario combinations. It has clearly shown that the proposed method is advantageous in all terms expect for computation time. Cases with the fixed battery degradation cost lead to the worst results as its averaged degradation cost and the discharge ratio are both the highest, which means the battery may be inappropriately exploited. On the other side, cases with the piece-wise linear cost models produces very similar results with the proposed model with higher costs and discharge ratio and lower computation time, while cases with the quadratic

TABLE V
RESULTS OF COMPARATIVE CASES

Result	I-A	I-B	I-C	II-A	II-B	II-C	III-A	III-B	III-C	IV-A	IV-B	IV-C	V-A	V-B	V-C
Operational cost ($)	0.2935	0.4123	0.2946	0.2931	0.5011	0.3122	0.2983	0.4512	0.3129	0.3001	0.4339	0.3102	0.3123	0.4722	0.3270
Batt degradation cost ($)	0.00934	0.03432	0.01642	0.01462	0.06123	0.02046	0.01236	0.03985	0.01936	0.01132	0.03712	0.01712	0.01356	0.03832	0.01397
Discharge ratio* (%)	66.34	172.62	89.12	92.36	201.63	111.36	73.26	182.46	94.17	74.12	181.29	81.99	86.42	182.93	101.12
Computation time† (s)	47.556	17.56	306.332	9.563	3.724	126.442	21.429	7.436	152.357	26.462	11.423	171.939	31.437	16.443	193.462

*: Discharge ratio is calculated by adding the DOD of all discharging events and then averaging in 24 hours.

†: Computation time is counted for searching the optimal results in the time interval of upper layer.

cost merely takes the average result with even worse DOD ratio and computation time ratings.

Compared with the nonlinear model for degradation costs, one of the major shortcomings of fixed, piecewise linear and quadratic cost models is they cannot effectively reduce the charging and discharging frequency, as illustrated by row 4 (discharge ratio) in Table V . This is because the cost is directly linked with the exchange power of energy storage as a constant approximation in spite of its operating conditions, resulting to the fact that SOC and DOD have little relationship with the real-time degradation process. On the other hand, by comparing the results of scenario III and IV, it can be observed that the accuracy of such approximation methods is very dependent on the sampling points, which may in turn affect the optimization performance if the sampling points are not carefully selected. On the contrary, the nonlinear degradation model provides more levels of detail and ultimately reduces the charging/discharging frequency since it is derived directly from the characteristics of different energy storages. Therefore, the nonlinear degradation cost model can provide the most accurate and effective results.

As for the algorithms, it can be also seen in Table V that the formulation of a single-layer optimization problem may be insufficient to make appropriate power dispatch for hybridized ESS with distinctive characteristics, especially for battery and supercapacitor in this case. It can be seen that the single-layer model in I-C has encountered the computation issue since the optimization problem cannot be solved within the predefined time interval (5 min). It is difficult to make scheduling for supercapacitor in the long time scale such as one hour due to its lower energy density, and likewise, frequent charging and discharging for battery in short term deteriorate the lifetime dramatically, which may be not beneficial for long-term economic operation. To this end, the time interval for the single-layer model must be carefully selected to fit the need of hybridized ESS, especially for the supercapacitor rather than battery. However, this may affect the result accuracy in turn. Therefore, one single layer optimization may not address the functionality of hybridization of energy storages, and its validity of single-layer optimization structure may be questioned by such the compromise between prediction horizon and computational burden. On the contrary, the design of such a two-layer structure in the paper is specifically tailored to divide operation modes into variant time scales to deal with different characteristics of energy storages, at the expense of the computational time. With high-performance computer and more advanced solvers, the computation speed can be speed-up significantly.

VI. CONCLUSION

In this paper, a two-layer EMS for microgrids with the hybrid ESS considering degradation cost models is proposed. We model the problem in the way that minimization of the operational cost is achieved while the power fluctuation by RES is accounted for. Degradation cost models of battery and supercapacitor are developed to convert the long-term capital cost into short-term operation problems. The two-layer EMS with hybrid ESS is proposed in accordance with the degradation cost models, in which power dispatch is scheduled to minimize the operational cost in the upper layer and power fluctuations by RES forecast errors are minimized in the lower layer. The proposed EMS is applied to a microgrid which includes the PCC to the utility grid, a hybrid ESS, a RES system and the aggregate load. Simulation studies successfully demonstrate that different types of energy storages including batteries and supercapacitors can be utilized at different layers for multiple decision-making objectives. Scenarios incorporating pricing schemes, prediction horizon lengths and forecast accuracies prove effectiveness of the proposed two-layer EMS structure. In the future work, stochastic programming will be considered to incorporate with the proposed EMS and uncertainties in RES forecasting and RES generation output will be modeled.

REFERENCES

[1] K. Rahbar, X. Jie, and Z. Rui, "Real-time energy storage management for renewable integration in microgrid: An off-line optimization approach," *IEEE Trans. Smart Grid*, vol. 6, no. 1, pp. 124–134, 2015.

[2] A. Tani, M. B. Camara, and B. Dakyo, "Energy management in the decentralized generation systems based on renewable energyultracapacitors and battery to compensate the wind/load power fluctuations," *IEEE Trans. Ind. Appl.*, vol. 51, no. 2, pp. 1817–1827, 2015.

[3] J. Shen and A. Khaligh, "A supervisory energy management control strategy in a battery/ultracapacitor hybrid energy storage system," *IEEE Trans. Transport. Electrific.*, vol. 1, no. 3, pp. 223–231, 2015.

[4] J. Xiao, P. Wang, and L. Setyawan, "Hierarchical control of hybrid energy storage system in dc microgrids," *IEEE Trans. Ind. Electron.*, vol. 62, no. 8, pp. 4915–4924, 2015.

[5] N. Mendis, K. M. Muttaqi, and S. Perera, "Management of battery-supercapacitor hybrid energy storage and synchronous condenser for isolated operation of pmsg based variable-speed wind turbine generating systems," *IEEE Trans. Smart Grid*, vol. 5, no. 2, pp. 944–953, 2014.

[6] Q. Xie, Y. Wang, Y. Kim, M. Pedram, and N. Chang, "Charge allocation in hybrid electrical energy storage systems," *IEEE Trans. Comput.-Aided Design Integr. Circuits Syst.*, vol. 32, no. 7, pp. 1003–1016, 2013.

[7] Y. Ghiassi-Farrokhfal, C. Rosenberg, S. Keshav, and M. B. Adjaho, "Joint optimal design and operation of hybrid energy storage systems," *IEEE J. Sel. Areas Commun.*, vol. 34, no. 3, pp. 639–650, 2016.

[8] M. E. Choi, S. W. Kim, and S. W. Seo, "Energy management optimization in a battery/supercapacitor hybrid energy storage system," *IEEE Trans. Smart Grid*, vol. 3, no. 1, pp. 463–472, 2012.

[9] M. Yazdanian and A. Mehrizi-Sani, "Distributed control techniques in microgrids," *IEEE Trans. Smart Grid*, vol. 5, no. 6, pp. 2901–2909, 2014.

[10] C. Zhang, Y. Xu, Z. Y. Dong, and J. Ma, "Robust operation of microgrids via two-stage coordinated energy storage and direct load control," *IEEE Trans. Power Syst.*, vol. PP, no. 99, pp. 1–1, 2016.

[11] D. E. Olivares, C. A. Caizares, and M. Kazerani, "A centralized energy management system for isolated microgrids," *IEEE Trans. Smart Grid*, vol. 5, no. 4, pp. 1864–1875, 2014.

[12] H. Kanchev, L. Di, F. Colas, V. Lazarov, and B. Francois, "Energy management and operational planning of a microgrid with a pv-based active generator for smart grid applications," *IEEE Trans. Ind. Electron.*, vol. 58, no. 10, pp. 4583–4592, 2011.

[13] S. Grillo, M. Marinelli, S. Massucco, and F. Silvestro, "Optimal management strategy of a battery-based storage system to improve renewable energy integration in distribution networks," *IEEE Trans. Smart Grid*, vol. 3, no. 2, pp. 950–958, 2012.

[14] M. N. Mojdehi and P. Ghosh, "Estimation of the battery degradation effects on the ev operating cost during charging/discharging and providing reactive power service," in *2015 IEEE 81st Vehi. Tech. Conf.*, 2015, Conference Proceedings, pp. 1–5.

[15] K. Worthmann, C. M. Kellett, P. Braun, L. Grune, and S. R. Weller, "Distributed and decentralized control of residential energy systems incorporating battery storage," *IEEE Trans. Smart Grid*, vol. 6, no. 4, pp. 1914–1923, 2015.

[16] A. Parisio, E. Rikos, and L. Glielmo, "A model predictive control approach to microgrid operation optimization," *IEEE Trans. Control Syst. Technol.*, vol. 22, no. 5, pp. 1813–1827, 2014.

[17] O. Ozel, K. Shahzad, and S. Ulukus, "Optimal energy allocation for energy harvesting transmitters with hybrid energy storage and processing cost," *IEEE Trans. Signal Process.*, vol. 62, no. 12, pp. 3232–3245, 2014.

[18] X. Ke, N. Lu, and C. Jin, "Control and size energy storage systems for managing energy imbalance of variable generation resources," *IEEE Trans. Softw. Eng.*, vol. 6, no. 1, pp. 70–78, 2015.

[19] A. Fakhrazari, H. Vakilzadian, and F. F. Choobineh, "Optimal energy scheduling for a smart entity," *IEEE Trans. Smart Grid*, vol. 5, no. 6, pp. 2919–2928, 2014.

[20] "Energy market company (emcsg)," 2015. [Online]. Available: https://www.emcsg.com/marketdata

[21] K. W. Wee, S. S. Choi, and D. M. Vilathgamuwa, "Design of a least-cost battery-supercapacitor energy storage system for realizing dispatchable wind power," *IEEE Trans. Sustain. Energy*, vol. 4, no. 3, pp. 786–796, 2013.

[22] M. Koller, T. Borsche, A. Ulbig, and G. Andersson, "Defining a degradation cost function for optimal control of a battery energy storage system," in *2013 IEEE PowerTech*, 2013, pp. 1–6.

[23] P. P. Varaiya, F. F. Wu, and J. W. Bialek, "Smart operation of smart grid: Risk-limiting dispatch," *Proc. IEEE*, vol. 99, no. 1, pp. 40–57, 2011.

[24] Y. Lei, C. Xu, Z. Junshan, and H. V. Poor, "Cost-effective and privacy-preserving energy management for smart meters," *IEEE Trans. Smart Grid*, vol. 6, no. 1, pp. 486–495, 2015.

[25] K. Smith, M. Earleywine, E. Wood, and A. Pesaran, "Battery wear from disparate duty-cycles: Opportunities for electric-drive vehicle battery health management," in *2012 Amer. Contr. Conf.*, Montreal, Canada, 2012, Conference Proceedings.

[26] J. Vetter, P. Novk, M. R. Wagner, C. Veit, K. C. Mller, J. O. Besenhard, M. Winter, M. Wohlfahrt-Mehrens, C. Vogler, and A. Hammouche, "Ageing mechanisms in lithium-ion batteries," *J. Power Sour.*, vol. 147, no. 12, pp. 269–281, 2005. [Online]. Available: http://www.sciencedirect.com/science/article/pii/S0378775305000832

[27] S. Drouilhet and B. Johnson, "A battery life prediction method for hybrid power applications preprint," 1997.

[28] C. Zhou, K. Qian, M. Allan, and W. Zhou, "Modeling of the cost of ev battery wear due to v2g application in power systems," *IEEE Trans. Energy Convers.*, vol. 26, no. 4, pp. 1041–1050, 2011.

[29] H. Farzin, M. Fotuhi-Firuzabad, and M. Moeini-Aghtaie, "A practical scheme to involve degradation cost of lithium-ion batteries in vehicle-to-grid applications," *IEEE Trans. Softw. Eng.*, vol. 7, no. 4, pp. 1730–1738, 2016.

[30] S. Han, S. Han, and H. Aki, "A practical battery wear model for electric vehicle charging applications," *Appli. Energ.*, vol. 113, pp. 1100–1108, 2014.

[31] G. Alcicek, H. Gualous, P. Venet, R. Gallay, and A. Miraoui, "Experimental study of temperature effect on ultracapacitor ageing," in *Proc. 2007 Eur. Conf. on Power Electron. and Appl.*, 2007, pp. 1–7.

[32] D. Linzen, S. Buller, E. Karden, and R. W. De Doncker, "Analysis and evaluation of charge-balancing circuits on performance, reliability, and lifetime of supercapacitor systems," *IEEE Trans. Ind. Appl.*, vol. 41, no. 5, pp. 1135–1141, 2005.

[33] P. Kreczanik, P. Venet, A. Hijazi, and G. Clerc, "Study of supercapacitor aging and lifetime estimation according to voltage, temperature, and rms current," *IEEE Trans. Ind. Electron.*, vol. 61, no. 9, pp. 4895–4902, 2014.

[34] M. Ayadi, O. Briat, R. Lallemand, A. Eddahech, R. German, G. Coquery, and J. M. Vinassa, "Description of supercapacitor performance degradation rate during thermal cycling under constant voltage ageing test," *Microelectron. Reliab.*, vol. 54, no. 910, pp. 1944–1948, 2014.

[35] A. Oukaour, B. Tala-Ighil, M. AlSakka, H. Gualous, R. Gallay, and B. Boudart, "Calendar ageing and health diagnosis of supercapacitor," *Electr. Pow. Syst. Res.*, vol. 95, pp. 330–338, 2013.

[36] H. Nafisi, S. M. M. Agah, H. A. Abyaneh, and M. Abedi, "Two-stage optimization method for energy loss minimization in microgrid based on smart power management scheme of phevs," *IEEE Trans. Smart Grid*, vol. 7, no. 3, pp. 1268–1276, 2016.

[37] W. Hu, P. Wang, and H. Gooi, "Towards optimal energy management of microgrids via robust two-stage optimization," *IEEE Trans. Smart Grid*, vol. PP, no. 99, pp. 1–1, 2016.

[38] Y. Zhang, R. Wang, T. Zhang, Y. Liu, and B. Guo, "Model predictive control-based operation management for a residential microgrid with considering forecast uncertainties and demand response strategies," *IET Gener. Transm. Distrib.*, vol. 10, no. 10, pp. 2367–2378, 2016.

[39] A. Wchter and L. T. Biegler, "On the implementation of an interior-point filter line-search algorithm for large-scale nonlinear programming," *Math. Prog.*, vol. 106, no. 1, pp. 25–57, 2006. [Online]. Available: http://dx.doi.org/10.1007/s10107-004-0559-y

[40] I. Gurobi Optimization, "Gurobi optimizer reference manual," 2016. [Online]. Available: http://www.gurobi.com

[41] W. G. Pell, B. E. Conway, W. A. Adams, and J. de Oliveira, "Electrochemical efficiency in multiple discharge/recharge cycling of supercapacitors in hybrid ev applications," *J. Power Sour.*, vol. 80, no. 1, pp. 134–141, 1999.

[42] P. Rodatz, G. Paganelli, A. Sciarretta, and L. Guzzella, "Optimal power management of an experimental fuel cell/supercapacitor-powered hybrid vehicle," *Control Eng. Prac.*, vol. 13, no. 1, pp. 41–53, 2005.

[43] B. Xu, A. Oudalov, A. Ulbig, G. Andersson, and D. Kirschen, "Modeling of lithium-ion battery degradation for cell life assessment," *IEEE Trans. Smart Grid*, vol. PP, no. 99, pp. 1–1, 2016.

Chengquan Ju received the B.Eng. degree in electrical engineering from Wuhan University, Wuhan, China, in 2012 and the M.Sc degree in power engineering from Nanyang Technological University (NTU), Singapore, in 2013. He is currently pursuing the Ph.D. degree in the Energy Research Institute, NTU, Singapore. His research interests include energy management, optimal power flow, energy storage planning, hybrid energy system and hierarchical control in microgrid.

Peng Wang (M'00–SM'11) received the B.Sc. degree from Xi'an Jiaotong University, Xian, China, in 1978, the M.Sc. degree from the Taiyuan University of Technology, Taiyuan, China, in 1987, and the M.Sc. and Ph.D. degrees in power engineering from the University of Saskatchewan, Saskatoon, SK, Canada, in 1995 and 1998, respectively. He is currently a full Professor with the School of Electrical and Electronic Engineering, Nanyang Technological University, Singapore. His research interests include power system planning and operation, renewable energy planning, solar/electricity conversion system and power system reliability analysis.

Lalit Goel (F'13) received the B.Tech. degree from the Regional Engineering College, Warangal, India, in 1983, and the M.Sc. and Ph.D. degrees in electrical engineering from the University of Saskatchewan, Saskatoon, SK, Canada, in 1988 and 1991, respectively. He joined the School of Electrical and Electronic Engineering at the Nanyang Technological University, Singapore, in 1991, where he is currently a Professor of Power Engineering and Director of the Office of Global Education and Mobility.

Yan Xu (S'10-M'13) received the B.Eng. and M.Eng. degrees from South China University of Technology, China, in 2008 and 2011, respectively, and the Ph.D. degree from the University of Newcastle, Australia, in 2013. He was a Research Fellow with the Center for Intelligent Electricity Networks at the University of Newcastle from 2013 to 2014. He is currently an Assistant Professor with the School of Electrical and Electronic Engineering, Nanyang Technological University, Singapore. His research interests include power system stability and control, microgrid and multi-energy network, intelligent system and its applications to power engineering.